

14.8 ANALYTICAL METHODS

This section contains historical information for the initial operating cycle of Browns Ferry Units 1, 2, and 3. The current methodology is discussed in Section 14.6.

14.8.1 Nuclear Excursion Analysis

14.8.1.1 Introduction

Although extensive preventative measures in the forms of equipment design and procedural controls are taken to avoid nuclear excursions, such an event is assumed as a design basis accident. A continued effort is made in the area of analytical methods to assure that nuclear excursion calculations reflect the state of the art in the field. This section outlines only the broader aspects of the subject. Greater detail is available in technical literature.¹

14.8.1.2 Description

There are many ways of inserting reactivity into a large-core boiling water reactor. However, most of them result in a relatively slow rate of reactivity insertion and therefore pose no threat to the system. The one category of reactivity additions that must be considered in evaluating large nuclear excursions is that associated with the control rod system. It appears, at this time, that the rapid removal of a high-worth control rod is the only way of obtaining a high enough rate of reactivity insertion to result in a potentially significant excursion.

The rapid removal of a high-worth rod results in a high local reactivity in a small region of the core. For large, loosely coupled cores, this would result in a highly peaked power distribution and subsequent shutdown mechanisms. Significant shifts in the spatial power generation would occur during the course of the excursion; therefore, the method of analysis must be capable of properly accounting for any possible effects of the power distribution shifts. This is an effect which is not significant in small cores.

With this background in mind, it is now possible to categorize nuclear excursions in water-moderated, oxide cores. The categorization criterion that seems most definitive is one based on the principal shutdown mechanisms that come into play. This method is particularly useful here because for fuel such as that in the current General Electric product line reactors, the principal shutdown mechanisms have a direct relationship to both the consequences of the excursion and the

1 Wood, J. E.: "Analysis Methods of Hypothetical Super-Prompt Critical Reactivity Transients in Large Power Reactors," General Electric Company, Atomic Power Equipment Department, April 1968 (APED-5448).

applicable method of analysis. With respect to the energy densities presented, the following reference points are used:

Enthalpy = 0 cal/gm at ambient temperature,
Enthalpy = 220 cal/gm at incipient melting of UO_2 ,
Enthalpy = 280 cal/gm at fully-molten UO_2 , and
Enthalpy = 425 cal/gm when UO_2 vapor pressure is 1000 psi.

Table 14.8-1 describes the three categories of nuclear excursions, assuming a very low initial power level. As shown in Table 14.8-1, there is some overlap in the three ranges of excursions. The indicated numbers for reactivity insertion rate, minimum period, and peak energy density are nominal values and will vary somewhat from one reactor to another.

In the low reactivity insertion rate range, the reactor is barely prompt critical, and the energy that is stored in the fuel as a result of the nuclear burst is built up at a relatively slow rate. As a result, there may be a significant amount of heat transfer out of the fuel during the burst, and the negative moderator coefficient as well as the U-238 Doppler effect contributes to the shutdown mechanisms. In the medium range, the period is much shorter, and there is very little heat transfer out of the fuel during the burst. In this case, the principal shutdown mechanism is the Doppler effect. Finally, in the high range, there exists the possibility of core disassembly during the burst, due to high internal pressure causing prompt failure of fuel rods. This results in a significant contribution toward shutdown of the excursion.

In terms of consequences, the low range is limited to no fuel cladding damage, or at worst, a small amount of burnout. This poses no threat to nuclear system integrity; therefore, from a safety viewpoint, only the medium and high ranges are considered. The design basis rod drop accident is in the medium range, well below the range where core disassembly is possible.

14.8.2 Reactor Vessel Depressurization Analysis

This section contains descriptions of the analytical methods utilized to analyze accidents for the initial operating cycle. The bounding analysis has been reanalyzed by NEDC-32484P, Revision 1 and its associated references. The following original information is retained in this section for historical purposes.

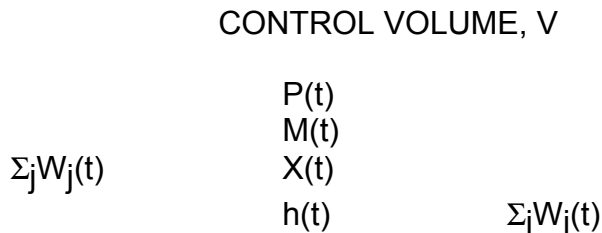
14.8.2.1 Introduction

The analytical methods used to calculate the energy and mass release rates issuing from a reactor vessel during rapid depressurization are described in this section. Conservation of mass and energy equations are written for a constant-volume system containing saturated steam and liquid in thermodynamic equilibrium to determine the thermodynamic state in the vessel. Mass flow rates into and out of

the vessel are then used to find the rate of change of system pressure and mass inventory.

14.8.2.2 Theoretical Development

The mathematical formulation for the depressurization of the reactor vessel can be derived by considering the conservation of mass and energy in the constant-volume system during rapid depressurization as shown in the control volume sketch below. If the mass flow rates are known it is possible to develop expressions of the rate of change of mass, energy, and pressure within the system.



14.8.2.2.1 Mass Balance

The volume of the control system is comprised of saturated liquid and saturated vapor in equilibrium:

$$V = M_f v_f + M_g v_g = \text{constant}, \quad (14.1)$$

where:

V = Total volume of the system (i.e., the reactor vessel)
v = Specific volume, and
M = Mass.

(The subscripts f and g refer to the liquid and vapor phases, respectively.)

Since the total mass in the system is simply

$$M = M_f + M_g \quad (14.2)$$

then the steam quality by weight, is given as,

$$X = \frac{M_g}{M} \quad (14.3)$$

14.8.2.2.2 Mass Rate of Change in Vessel

From continuity the rate of change of vapor mass in the system is equal to the net inflow of vapor plus the rate at which liquid is flashed to vapor due to depressurization. Hence,

$$\frac{dM_g}{dt} = \sum_j w_{g_j} - \sum_i w_{g_i} + W_{fg} \quad (14.4)$$

where:

w = mass flow rate

W_{fg} = net flashing rate.

(The subscript j corresponds to inflow while i refers to the outflow from the vessel evaluated at the thermodynamic conditions within the system.) Similarly, the rate of change of liquid mass in the vessel is

$$\frac{dM_f}{dt} = \sum_j w_{f_j} - \sum_i w_{f_i} - W_{fg} \quad (14.5)$$

14.8.2.2.3 Rate of Change of Energy in Vessel

The rate of change of energy in the system can be expressed from the First Law of Thermodynamics:

(Net energy inflow) - (net energy outflow) = (rate of change of internal energy)

$$\left(\dot{q} + \sum_j w_f h_f + \sum_j w_g h_g \right) - \left(\sum_i w_f h_f + \sum_i w_g h_g \right) = \frac{d}{dt} (M_f h_f + M_g h_g - VP) \quad (14.6)$$

where:

h = Enthalpy,
 P = Saturated pressure in the system, and
 \dot{q} = Heat transfer rate to the fluid from the surroundings (solids).

The right hand side of Equation (14.6) can be expanded; using the chain rule, to yield

(Rate of change of internal energy)

$$= \left[M_g \frac{dh_g}{dP} + M_f \frac{dh_f}{dP} \right] \frac{dP}{dt} + h_g \frac{dM_g}{dt} + h_f \frac{dM_f}{dt} - V \frac{dP}{dt} \quad (14.6a)$$

14.8.2.2.4 Flashing Rate in Vessel

After substituting Equations (14.4), (14.5), and (14.6a) into Equation (14.6), the expression for the net flashing rate is:

$$\begin{aligned}
 W_{f_g} = & \frac{1}{h_{f_g}} \dot{q} + \sum_j w_g h_g - \left(\sum_j w_g \right) h_g + \sum_j w_f h_f \\
 & - \left(\sum_j w_f \right) h_f - \left[M_g \frac{dh_g}{dP} + M_f \frac{dh_f}{dP} - V \right] \frac{dP}{dt} \quad (14.7)
 \end{aligned}$$

14.8.2.2.5 Vessel Depressurization Rate

In order to arrive at an expression for depressurization rate, we start by differentiating Equation (14.1), realizing that for a fixed total system volume $dV/dt = 0$; then,

$$M_g \frac{dv_g}{dt} + v_g \frac{dM_g}{dt} + M_f \frac{dv_f}{dt} + v_f \frac{dM_f}{dt} = 0 \quad (14.8)$$

BFN-18

Now expanding this by means of the chain rule we obtain:

$$v_g \frac{dM_g}{dt} + v_f \frac{dM_f}{dt} + \left(M_f \frac{dv_f}{dP} + M_g \frac{dv_g}{dP} \right) \frac{dP}{dt} = 0 \quad (14.9)$$

With expressions for dM_g/dt and dM_f/dt as given in Equations (14.4) and (14.5), Equation (14.9) can be written:

$$v_g \left[\sum_j w_g - \sum_i w_g + w_{fg} \right] \quad (14.10)$$

$$+ v_f \left[\sum_j w_f - \sum_i w_f - w_{fg} \right] + \left[M_f \frac{dv_f}{dP} + M_g \frac{dv_g}{dP} \right] \frac{dP}{dt} = 0$$

After substituting Equation (14.7) into Equation (14.10) and rearranging, the following expression for depressurization rate is obtained:

$$\frac{dP}{dt} = - \left[\frac{f_1(P) + f_2(P)}{f_3(P)} \right] \quad (14.11)$$

where:

$$f_1(P) = v_f \left(\sum_j w_f - \sum_i w_f \right) + v_g \left(\sum_j w_g - \sum_i w_g \right)$$

$$f_2(P) =$$

$$\frac{v_{fg}}{h_{fg}} \left[\dot{q} + \sum_j w_f h_f - \left(\sum_j w_f \right) h_f + \sum_j w_g h_g - \left(\sum_j w_g \right) h_g \right]$$

$$f_3(P) = M_g \left[\frac{dv_g}{dP} - \left(\frac{v_{fg}}{h_{fg}} \right) \frac{dh_g}{dP} \right]$$

$$+ M_f \left[\frac{dv_f}{dP} - \left(\frac{v_{fg}}{h_{fg}} \right) \frac{dh_f}{dP} \right] + \left(\frac{v_{fg}}{h_{fg}} \right) \frac{V}{J}$$

$$J = 778 \text{ ft lbs (enthalpy)/Btu}$$

14.8.2.2.6 Mass Flow Rates

The mass flow rates entering the reactor vessel during the blowdown are treated as functions of time and are independent of the internal thermodynamic conditions in the vessel. These flow rates can be liquid or vapor or some combination of the two. The outlet flow rate can be calculated from one of two flow models: critical flow as a function of the control volume stagnation properties P_o and h_o , or supercritical flow as a function of the pressure difference $P_o - P_{\text{sink}}$ (sink refers to the pressure outside the vessel).

Critical flow is flow which is "choked" at some point where the Mach number is unity in the line through which depressurization is taking place. Critical or maximum flow (both single-phase and two-phase) persists when the ratio of driving pressure (vessel pressure) to sink pressure (drywell) is greater than approximately two. The critical flow analysis of F. J. Moody² is used to determine the flow rate for critical flow conditions.

For the instantaneous values of pressure, P , enthalpy, h , and friction coefficient, f , L/d , a three-variable interpolation is performed using Moody's results to find the critical mass velocity:

$$G_c = G(P, h, \bar{f}L / d) \quad (14.12)$$

The mass flow rate is now calculated from

$$w_c = AG_c, \quad (14.13)$$

where:

A = minimum flow area in the line.

Supercritical flow will exist prior to the formation of bubbles in a liquid flow and establishment of two-phase critical flow, or when the source pressure is low so that the ratio of $P_o / P_{\text{sink}} < 2$.

Supercritical mass velocity is calculated from:

2 Moody, F. J.: "Maximum Two-Phase Vessel Blowdown from Pipes," General Electric Company, Atomic Power Equipment Department, April 1965 (APED-4827).

$$G_{sc} = \frac{2g(P_o - P_{sink})}{v_f (1.4 + fL/d)^2 \Phi} \quad (14.14)$$

where:

Φ = Martinelli-Nelson two-phase multiplier.³

The mass flow rate is:

$$W_{sc} = A G_{sc} \quad (14.15)$$

14.8.2.3 Numerical Solution

If a function of time and its time derivatives are known at time t_1 , then the value of the function at time $t_1 + \Delta t$ can be obtained from a Taylor series expansion. The first three terms of the series are:

$$f(t_1 + \Delta t) = f(t_1) + \frac{\Delta t}{1!} f'(t_1) + \frac{\Delta t^2}{2!} f''(t_1) + \dots, \quad (14.16)$$

where:

$$f'(t_1) = \frac{df}{dt} \text{ at } t = t_1$$

$$f''(t_1) = \frac{d^2 f}{dt^2} \text{ at } t = t_1 \text{ and}$$

$$\Delta t = \text{Size of time step.}$$

Integration - If the term involving the second derivative is negligible, the Euler forward integration method is obtained

$$f(t_1 + \Delta t) = f(t_1) + \Delta t f'(t_1) \quad (14.17)$$

Time Step - A variable time step based on an accuracy criterion has been used in the integration method. The error made in one extrapolation of the Euler method

3 Martenelli, R. C. and Nelson, D. B., "Prediction of Pressure Drop During Forced-Circulation Boiling Water," Trans. ASME, Vol. 70, 1948, p. 695.

BFN-18

can be approximated by the third term of Taylor's series given by Equation (14.16); i.e.,

$$e \approx \frac{\Delta t^2}{2!} f''(t_1) \quad (14.18)$$

An exact equation for the second time derivative can be approximated by the rate of change of the first derivative; i.e.,

$$f''(t_1) = \frac{f'(t_1 + \Delta t) - f'(t_1)}{\Delta t} \quad (14.19)$$

After substituting Equations (14.10) into (14.18), an approximation of the error made in one time step can be calculated:

$$e \approx \frac{\Delta t}{2} | f'(t_1 + \Delta t) - f'(t_1) | \quad (14.20)$$

If the magnitude of this error is within the error criterion, then the time step is doubled for the next calculation. If $|e| > \epsilon$, then the time step is halved and the previous calculations are repeated.

Calculations - Equations (14.4), (14.5), and (14.11) are programmed for machine calculation using the numerical methods described above.

14.8.3 Reactor Core Heatup Analysis

This section contains descriptions of the analytical methods utilized to analyze accidents for the initial operating cycle. The bounding analysis has been reanalyzed by NEDC-32484P, Revision 1 and its associated references. The following original information is retained in this section for historical purposes.

14.8.3.1 Introduction

The analytical method used to calculate the reactor core thermal transient following a loss-of-coolant accident is described in this section. The fuel temperature, cladding temperature, channel temperature, and amount of metal-water reaction are calculated as functions of time from the start of the accident. In this analysis the power of decaying fission products, the chemical energy released by metal-water

reactions, and the stored heat in the fuel, cladding, and other metal in the core are included as heat sources.

The fuel rods are classified such that those with similar power levels and fuel bundle locations are analyzed as a group. A one-dimensional heat balance is then written for each type of fuel rod. Heat is transferred from the surface of the fuel rods by convection to the water, steam or hydrogen formed in the metal-water reaction. In addition, thermal radiation between fuel rods and from the rods to the channel is accounted for in the overall heat balance.

14.8.3.2 Theoretical Development

A typical fuel rod consists of uranium dioxide fuel with a Zircaloy cladding. An initial core fuel bundle consists of 49 fuel rods, grouped together to form a square array which is surrounded by a metal channel. The fuel rods are divided into four radial temperature zones for the numerical calculations as shown in Figure 14.8-1. The cladding, on the other hand, is described by the average cladding temperature, with an outer surface temperature computed from the average temperature. The channel (Figure 14.8-1) is considered to be at a uniform temperature radially. The fuel rods within the channel are divided into four representative zones to describe the spatial variation of power generation. The entire reactor core is made up of several hundred fuel bundles and channels. To describe the radial variations of power generation, the core is divided into five radial zones. The fuel rods and channels are divided into five axial regions. Axial conduction between regions is neglected. Each channel is considered to be isolated from the rest of the core so that interactions between adjacent channels is neglected.

14.8.3.2.1 Heat Sources.

The energy generated by delayed neutrons and decaying fission products is assumed to be uniform within a fuel rod and to have the same radial and axial variation within the core as the steady-state power distribution. The chemical energy released by the metal-water reaction is described by the parabolic rate law given by Baker⁴, where the rate of change of the metal oxide thickness is written as

$$\frac{d\delta}{dt} = \frac{K}{\delta} \exp (D / T_c) \quad (14.21)$$

where:

K = Rate coefficient,

4 Baker, L. J, and Avins, R. O.: "Analyzing the Effects of a Zirconium-Water Reaction," Nucleonics, 23(7), 70-74 (July 1965).

T_c = Cladding temperature,
 D = Activation coefficient, and
 δ = Oxide thickness

The heat generation rate and hydrogen release rate are proportional to the rate of change of oxide generated. The chemical heat liberated is given as follows:

$$\frac{dQ_c}{dt} = \frac{d\delta}{dt} \Delta H \rho_c A_s \quad (14.22)$$

where:

H = Heat of reaction,
 ρ_c = Density of metal, and
 A_s = Exposed surface area of oxide.

The mass rate of hydrogen generated is

$$\frac{dW_H}{dt} = 2 \frac{d\delta}{dt} \rho_c A_s \frac{N_{H_2}}{N_{METAL}} \quad (14.23)$$

where:

W_H = Mass of hydrogen generated and
 N = Molecular weight.

The above reaction rate considers that there is an unlimited source of saturated steam available for the reaction. The empirical reaction constants, K and D , are based upon experimental data obtained under conditions where the metal and water are at the same temperature. Therefore, for Equation (14.21) to be correct the water must be heated to the cladding temperature. The energy required to heat this water is deducted from the total chemical energy added to the system.

14.8.3.2.2 Conduction Heat Transfer

The heatup analysis considers only radial conduction of heat from the fuel to the cladding surface. Axial conduction along the fuel rods or to support structures is neglected. Resistance to heat flow through the fuel-cladding gap is taken into account.

14.8.3.2.3 Convection Heat Transfer

Heat is transferred from the cladding and channel to the surrounding fluid by thermal radiation and convection. During the blowdown a convection heat transfer coefficient must be calculated. The water level is calculated from the mass inventory in the reactor vessel during the blowdown. If an axial node is covered with water or steam water mixtures, the heat transfer coefficient for that node is obtained from the Jens-Lottes correlation for boiling heat transfer:

$$h_B = \frac{e^{P/900}}{1.9} (Q_s)^{0.75} \quad (14.24)$$

where:

P = Reactor pressure
 Q_s = Surface heat flux

Equation (14.24) is used to describe the heat transfer coefficient if the calculated water level is above the center of the node. When water level drops below the center of the node, it is treated as being completely uncovered and the convective heat transfer rate diminishes to zero.

14.8.3.2.4 Radiation

Thermal radiation between fuel rods and the fuel channel box is permitted if they are not covered with water. To simplify calculations, the fuel rods are grouped into four groups. Figure 14.8-1 shows the channel configuration. Group 1 rods exchange radiation with Groups 2, 3, and 4 rods and the channel. Group 2 rods exchange radiation with Groups 1, 3, and 4 rods and the channel. Group 3 rods exchange radiation with Groups 1, 2, and 4 rods and the channels. Finally, Group 4 rods exchange radiation only with Groups 1, 2, and 3 rods. Radiation view factors are also calculated for each group of rods. The view factors together with the emissivity and relative areas are converted to radiation coefficients used in the Stephan-Boltzman equation for obtaining the radiant heat transfer.

14.8.3.3 Method of Solution

The fuel, cladding, and channel temperature are calculated at each time step by considering the aforementioned energy consideration. All temperatures are integrated using a simple Euler forward difference method:

$$\Phi(t + \Delta T) = \Phi(t) + \frac{d\Phi(t)}{dt} \Delta t \quad (14.25)$$

All physical properties are considered constant with temperature and time. The model utilizes the calculated histories of pressure, water level, and heat transfer coefficients. The sink temperature for all convective heat transfer calculations is determined by the saturation temperature at the given pressure.

14.8.4 Containment Response Analysis

This section contains descriptions of the analytical methods utilized to analyze accidents for the initial operating cycle. The bounding long-term pressure suppression pool analysis has been reanalyzed by NEDC-32484P, Revision 2, GE-NE-B13-01866-4, Revision 2 and their associated references. The following original information for the long-term pressure suppression pool analysis is retained in this section for historical purposes.

14.8.4.1 Short Term Containment Response

The analytical model used to evaluate the short term response of a pressure suppression containment to a loss-of-coolant accident consists of five submodels, i.e.,

1. Reactor vessel model,
2. Drywell model,
3. Vent clearing model,
4. Vent flow model, and
5. Pressure Suppression chamber model.

These submodels are described in detail in the topical report "The General Electric Pressure Suppression Containment Analytical Model," NEDO-10320, April 1971. Included in the report are all the assumptions used in the model as well as descriptions of experimental verification and a discussion of the degree of conservatism inherent in the calculated results.

14.8.4.2 Long Term Containment Pressure Response

The preceding analytical model is used to calculate the containment transient during the reactor vessel depressurization and during the containment depressurization

BFN-18

which follows the vessel transient. Once the depressurization is over (about 600 seconds after the accident), a considerably simplified model can be used. The key assumptions employed in the simplified model are:

- a. Drywell and pressure suppression chamber, both saturated and at the same total pressure,
- b. An energy balance is performed to determine the temperature of the emergency core cooling flow as it drains by gravity back into the pressure suppression chamber. The drywell is conservatively assumed to be 5°F hotter than the water draining back into the pressure suppression pool,
- c. The pressure suppression chamber air temperature is taken equal to the pool temperature which is determined from an energy balance on the pool mass, and
- d. No credit is taken for heat losses from the primary containment.

Since no mass is being added to the pressure suppression pool, the pool temperature can be calculated based on the following energy balance:

$$\dot{T}_s = \frac{h_D \dot{m}_{D_o} - h_s \dot{m}_{s_o} - \dot{q}_{H_x}}{M_{W_s}} \quad (14.26)$$

where:

- h_D = enthalpy of water leaving drywell
- \dot{m}_{D_o} = flow rate out of drywell
- h_s = enthalpy of water in pressure suppression chamber
- \dot{m}_{s_o} = flow rate out of pressure suppression chamber
- \dot{q}_{H_x} = heat removal rate of heat exchanger
- M_{W_s} = mass of water in pressure suppression chamber.

Assuming no storage in drywell

$$\dot{m}_{D_o} = \dot{m}_{s_o} = \dot{m}_{CSCS}$$

And since the only heat source is the core decay heat, we have:
Therefore,

BFN-18

$$(h_D - h_s) \dot{m}_{CSCS} = \dot{q}_D \quad (14.27)$$

$$\dot{T}_s = \frac{\dot{q}_D - \dot{q}_{H_x}}{M_{W_s}} \quad (14.28)$$

which can be integrated to give T as a function of time. At any point in time the drywell temperature is given by:

$$T_D = T_s + \frac{\dot{q}_D}{\dot{m}_{CSCS}} + 5^\circ \text{ F} \quad (14.29)$$

With the pressure suppression chamber and drywell temperatures known and their total pressures assumed equal, it is now possible to solve for the total pressure

$$\begin{aligned} P_D &= P_S \\ P_{aD} + P_{vD} &= P_{aS} + P_{vS} \\ \frac{M_{aD} R_{TD}}{V_D} + P_{vD} &= \frac{M_{aS} R_{TS}}{V_{vS}} + P_{vS} \quad (14.30) \end{aligned}$$

The total mass, M_T , can be determined from a mass balance on the primary containment:

$$\dot{M}_T = \dot{M}_{aD} + \dot{M}_{aS} = \dot{m}_i - \dot{m}_{LEAK} \quad (14.31)$$

where:

- \dot{m}_i = all noncondensable flow into containment, e.g., hydrogen from metal-water reaction, and
- \dot{m}_{LEAK} = leakage from primary containment.

Therefore, at any time, M_T , is known, and

$$M_T = M_{as} + M_{ad} \quad (14.32)$$

The two equations (14.30 & 14.32) can be solved for the two unknowns (M_{as} and M_{ad}) and the pressure determined.

The leakage rate from the primary containment is determined from the following relationship:

$$\dot{m}_{LEAK} = L_T \left[\frac{1 - \left(\frac{1}{p} \right)^2}{1 - \left(\frac{1}{P_T} \right)^2} \right]^{1/2} \quad (14.33)$$

where:

- L_T = Leak rate at test pressure
- P_T = Test pressure in absolute atmospheres
- P = Containment pressure in absolute atmospheres

The above equations are solved simultaneously on a step-by-step basis to obtain the long-term pressure transient of the primary containment.

14.8.5 Analytical Methods for Evaluating Radiological Effects

14.8.5.1 Introduction

This section describes the analytical techniques used to calculate the radiological exposures for design basis accidents. The descriptions following are retained for historical purposes only. The current descriptions for the radiological effects of design basis accidents are given in Sections 14.6 and 14.11.

Methods for evaluating external exposures from airborne fission products and internal exposures from inhalation of airborne radioactive materials are given.

The first portion of the analysis concerns the meteorological considerations that describe the dissemination of the radioactive material as it emanates from the source and spreads through the atmosphere. The second portion of the analysis describes the radiological effects on man as a result of the dispersed radioactive materials.

The radiological effects of the design basis accidents are evaluated at various discrete distances from the plant. The nearest distance is approximately the site boundary with other distances given to illustrate the change of the radiological effects with distance.

Since airborne materials are released via an elevated release point, the effects at short distances for any diffusion condition are usually much less for all modes of exposure except from the passing cloud. At these short distances, the plume has not yet reached ground level so that exposure from inhalation is small. The passing cloud effect, however, remains nearly constant due to essentially line-source geometry of the elevated plume.

14.8.5.2 Meteorological Diffusion Evaluation Methods

14.8.5.2.1 General

Six points in the atmospheric diffusion spectrum are used to evaluate the radiological effects of secondary containment leakage via the elevated release point. These points represent the meteorological conditions which could exist at the site.

The atmospheric diffusion methods are the same as those reported in the Journal of Applied Meteorology.⁵

14.8.5.2.2 Height of Release

Discharge from the secondary containment to the atmosphere emanates from the elevated release point. The effective height of release is the sum of the release point height plus any effluent rise due to momentum or buoyancy. For most of the design basis accidents, the additional effects of momentum and buoyancy are negligible, so that the effective release height is equal to the elevated release point height (183 meters). While buoyancy effects are significant for the steam line break accident, the conservative assumption is made that the release height is equal to the top of the turbine building.

14.8.5.2.3 Diffusion Conditions

An important parameter used in the atmosphere diffusion calculation is the measure of wind direction persistence and variability of direction. This parameter is the product of the standard deviation of the horizontal wind direction fluctuations, σ_{θ} and the average wind velocity \bar{u} . Combined with the assumed stability condition, specification of $\sigma_{\theta} \bar{u}$ permits calculation of air concentrations at various distances from the source.

A conservative value of 0.1 radian-meters/second is used for this parameter to describe the horizontal spreading of the plume for 1 meter/ second wind speed conditions. A value of 1.0 radian-meter/second is typical for a 5 meter/second condition. These values are typical for a one hour period. A choice of wind direction persistence (number of continuous hours) of 24 hours is used for poor diffusion conditions. This period is conservative when used with $\sigma_{\theta} \bar{u}$ of 0.1 radian-meter/ second and 1 meter/second wind speed, based upon the U.S. Weather Bureau Data shown in Table 14.8-2.⁶ Table 14.8-2 shows that wind persistency of periods as long as 24 hours occurs only about 0.1 percent of the time or less at the sites listed. The sites include flat terrain, coastal and lake shore sites and some valley locations. For a wind speed of 5 meters/second, a value of 1.0 radian-meters/second corresponds to a σ_{θ} of 0.20 radians which is similar to the value of 0.1 radians for the 1 meter/second case. Thus, about the same amount of

5 Fuguay, J. J., Simpson, C. L., and Hinds, W. T. "Prediction of Environmental Exposures from Sources Near the Ground Based on Hanford Experimental Data." Journal of Applied Meteorology, Vo. 3 No. 6, December 1964.

6 Pack, D. H., Angell, J. K., Van Der Hoven, I., and Slade, D. H., USWB, "Recent Developments in the Application of Meteorology to Reactor Safety," presented at the 1964 Geneva Conference, paper number A/CONF/28/P/714.

wind variability is considered and the conservative 24-hour persistence assumption is applicable to both cases.

14.8.5.2.4 Applied Meteorology

The diffusion and wind direction persistence conditions and breathing rates used for the design basis accident calculations are given in Table 14.8-3.

14.8.5.2.5 Cloud Dispersion Calculations

The dispersion of the released effluent is described by the Gaussian Diffusion Equation given below.

$$X / Q_o = \frac{f_d}{2p \sigma_y \sigma_z \bar{u}} e^{-\frac{1}{2} \left(\frac{y^2}{\sigma_y^2} + \frac{z^2}{\sigma_z^2} \right)} \quad (14.34)$$

where:

- X/Q_o = integrated air concentration (X) per unit activity release (Q_o)
- Y = distance from centerline crosswind (since plume centerline is used, $Y = 0$)
- z = height of plume above ground
- f_d = cloud depletion factor (halogens only) see paragraph 14.8.5.2.6
- σ_y = Horizontal diffusion coefficient
- σ_z = Vertical diffusion coefficient

σ_y and σ_z are defined as follows:

$$\sigma_y^2 = At - A\alpha + A\alpha e^{-t/a} \quad (\text{See footnote 5}) \quad (14.35)$$

where:

$$A = 13 + 232.5 (\sigma \theta \bar{u})$$

$$\alpha = \frac{A}{2 (\sigma \theta \bar{u})^2}$$

t = time after release and is $= x/\bar{u}$, where x is downwind distance.

The vertical cloud growth, as defined by the standard deviation of width σ_z is given by

$$\sigma_x^2 = a(1 - e^{-k^2 t^2}) + bt \quad (\text{stable case}) \quad (\text{See footnote 5}) \quad (14.36)$$

$$\sigma_z^2 = \frac{C_z^2 x^{(2-n)}}{2} \quad (\text{neutral / unstable case}) \quad (\text{See footnote 7}) \quad (14.37)$$

The values of the constants in Equations (14.36) and (14.37) are given below.

<u>Stability</u>	<u>Wind Speed (M/sec)</u>	<u>a</u> <u>(M²)</u>	<u>b</u> <u>(M²/sec)</u>	<u>k²</u> <u>(Sec⁻²)</u>
VS	1	3.4 x 10 ¹	2.5 x 10 ⁻²	8.8 x 10 ⁻⁴
U	1	-	-	-
U	5	-	-	-
N	1	-	-	-
N	5	-	-	-
MS	1	9.7 x 10 ¹	3.3 x 10 ⁻¹	2.5 x 10 ⁻⁴

<u>Stability</u>	<u>Wind Speed (M/sec)</u>	<u>C_z</u> <u>(M^{n/2})</u>	<u>n</u> <u>-</u>
VS	1	-	-
U	1	3.0 x 10 ⁻¹	2.0 x 10 ⁻¹
U	5	2.6 x 10 ⁻¹	2.0 x 10 ⁻¹
N	1	1.5 x 10 ⁻¹	2.5 x 10 ⁻¹
N	5	1.2 x 10 ⁻¹	2.5 x 10 ⁻¹
MS	1	-	-

The conventional "reflection" factor of 2 usually applied for releases from ground-level is not included. For the passing cloud dose, which is primarily a

gamma dose, the entire cloud volume is integrated as an "infinite" number of point sources to plus and minus infinity in the z-direction ignoring interception by the ground, so that the entire cloud volume is included. Inhalation doses are a function of concentration at the ground and subject to "reflection" effects if they exist. Since the materials of interest in inhalation effects deposit on the ground, "perfect" reflection will not occur, but rather the cloud will expand distorting the Gaussian mass distribution resulting in at most a small increase in concentration. In addition, no account is taken of the better diffusion near the ground compared to the stack exit elevation used. In any event, an increase by a factor of less than 2 but perhaps more than 1 may be a result of this "reflection" effect. A factor of 1.0 is used in this analysis.

No distinction in the choice of the diffusion parameter σ_z is made between the first two-hour period and the total accident dose calculations. This is inconsistent because larger values of this parameter are obviously appropriate for the longer time period. That is, the values used, as discussed in paragraph 14.8.5.2.3, are for one-hour periods, and thus are somewhat conservative when applied to the two-hour period dose calculation and are markedly conservative for the total accident calculation. Lack of data at this time for the longer time period does not permit more precise estimates to be made.

14.8.5.2.6 Cloud Depletion and Ground Deposition

The fallout concentrations of radioactive materials are determined on the basis of particle settling by eddy diffusion only, since settling by gravity is expected to be negligible in this case.

BFN-18

The extent of halogen and solid fission product deposition on the ground is a function of the apparent deposition velocity, which, in turn, is considered to be function of the diffusion condition and wind speed. Deposition velocities used in this evaluation are given below.⁷

<u>Meteorology</u>	<u>Wind Velocity (M/sec)</u>	<u>Deposition Velocity (cm/sec)</u>	
		<u>Noble Gases</u>	<u>Halogens</u>
Very stable	1	0	0.24
Moderately stable	1	0	0.34
Unstable	1	0	0.80
Unstable	5	0	4.00
Neutral	1	0	0.46
Neutral	5	0	2.30

These values of deposition velocity are used in the calculation of the cloud depletion term f_d .

$$f_d = \exp \left[- \frac{v_g}{u_o} \sqrt{\frac{2}{p}} \frac{u_o}{u_h} \int_0^t \frac{u_h \exp\left(\frac{-z^2}{2s_z^2}\right)}{s_z} dt \right] \quad (14.38)$$

where:

- f_d = Cloud depletion factor due to fallout
- V_g = Deposition velocity of isotope in question (cm/sec)
- u_o = Wind speed at ground level (cm/sec)
- u_h = Wind speed at height of release (cm/sec)
- σ_z = Vertical diffusion coefficient (cm)

14.8.5.2.7 Air Concentration Calculation

Using the equations developed above, the integrated air concentration from a release of 1 curie of activity is calculated in curie-seconds per cubic meter. These data are given in Tables 14.8-4 and 14.8-5 for the specified release heights and meteorological conditions.

⁷ Watson, E. C. and Gamertsfelder, C. C., "Environmental Radioactive Contamination as a Factor in Nuclear Plant Siting Criteria," HW-SA-2809, February 14, 1963.

14.8.5.3 Radiological Effects Calculation

The radiological doses of primary consideration are inhalation and cloud gamma. While the deposition gamma dose may be important from a decontamination viewpoint, it is of minor importance in evaluating the radiological consequences of a design basis accident and is, therefore, insignificant in this analysis.

The downwind radiological effects, such as cloud gamma and inhalation exposure, are a function principally of the integrated air concentration at any point. Calculation of this integrated concentration has been described in the preceding paragraphs. This paragraph describes the conversion of air concentration to radiation dose.

14.8.5.3.1 Passing Cloud Dose

The ground level whole body cloud gamma dose which is received from airborne radioactive materials is determined by summing the dose contribution from each incremental volume of air containing fission product activity. The dose from a point in space to a receptor located at coordinates X, Y, and Z is determined as follows:

$$D_g = \sum_{K=1}^m C_1 C_K f_K \int_{-\infty}^{\infty} \int_{-\infty}^{\infty} \int_{-\infty}^{\infty} X G_K dx dy dz \quad (14.39)$$

- D_g = Gamma dose at the receptor point (rem)
 C_1 = Conversion factor (3.7×10^{10} disintegrations/sec-curie)
 X = Integrated air concentration (curie-sec/m³)
 f_K = The number of photons of the Kth isotope released per disintegration (photons/dis)
 C_K = Flux to dose conversion factor. $\frac{\text{rem-m}^2}{\text{Sec-y}}$
 G_K = Dose attenuation kernel which is defined as follows

Where

$$G_K = B e^{-uT} / 4\pi T^2$$

Where

$$B = \text{Buildup factor} = 1 + KuT$$

$$K = \frac{u - u_a}{u a} \quad (14.40)$$

Where μ is the total absorption coefficient and μ_a is energy absorption coefficient (m^{-1})

$T =$ Distance from the source to the detector position and is equal to

$$\sqrt{x_1^2 + y_1^2 + z_1^2} \quad (14.41)$$

14.8.5.3.2 Inhalation Dose

The inhalation dose is an internal exposure which is received as a consequence of inhaling airborne radioactive fission products. Depending upon the isotopes inhaled there may be one or more organs which are affected.

The total activity inhaled during the inhalation period is

$$Q_{\text{dep.}} = \chi_i B_r \quad (14.42)$$

where:

- $\chi_i =$ Time integral of the air concentration previously defined in paragraph 14.8.5.2.7 (curie-sec/ m^3)
- $B_r =$ Breathing rate (m^3/sec)

When the above equation is multiplied by an appropriate conversion factor C_i (rem/sec-curie inhaled), a dose rate in the organ is obtained. The total dose resulting from inhalation of a mixture of fission products is

$$D_i = \sum_{i=1}^N \int_0^t c_i B_r C_i e^{-\lambda_i t} dt \quad (14.43)$$

Where

- $D_i =$ Total inhalation dose (rad)
- $\lambda_i =$ Effective decay constant of the i^{th} isotope in the organ of reference (sec^{-1})

The summation sign indicates that all isotopes contributing to the organ dose are added together to obtain the total inhalation dose.

BFN-18

The conversion factor C_i is applicable to the isotope of the organ of interest and is calculated by the use of the following mathematical model⁸

$$C_i = \frac{C_1 f_a E C_3}{M C_2} \quad (14.44)$$

- C_i = Activity to dose conversion factor (rad/sec-curie inhaled)
- C_1 = 1.6×10^{-6} ergs/MeV
- f_a = Fraction of inhaled material reaching the organ of reference
- E = The effective energy absorbed per disintegration MeV/dis)
- C_3 = 3.7×10^{10} dis/sec-curie
- M = Mass of the organ (gms)
- C_2 = 100 ergs/gm-rad

Therefore:

$$\begin{aligned} C_i &= \frac{(1.6 \times 10^{-6}) (f_a) (E) (3.7 \times 10^{10})}{(M) (100)} \\ &= \frac{5.92 \times 10^2 f_a E}{M} \quad (\text{rad / sec curie inhaled}) \quad (14.45) \end{aligned}$$

Upon integration of Equation (14.43), the total inhalation dose is

$$D_T = \sum_{i=1}^N \frac{c_i B_r C_i (1 - e^{-\lambda_i t})}{\lambda_i} \quad (14.46)$$

⁸ Morgan, K.A., Snyder, W. S. Auxier, J. A., "Report of the ICRP Committee II on Permissible Dose for Internal Radiation (1959)" Health Physics, Vol. 3 (1960).

BFN-18

If T is large compared to λ , Equation (14.46) can be simplified to

$$D_T = \sum_{i=1}^N \frac{c_i B_r C_i}{I_i} = \sum_{i=1}^N \frac{c_i B_r C_i T_i}{0.693} \quad (14.47)$$

Where:

T_i = Effective half life of the i^{th} isotope and is equal to

$$T_i = \frac{T_b T_r}{T_b + T_r}$$

T_b = Biological half life (sec)

T_r = Radioactive half life (sec)

If the effective half life is defined in terms of days and is combined with the conversion factor C'_i Equation (14.47) can be expressed follows

$$D_T = \sum_{i=1}^N c_i B_r C'_i \quad (14.48)$$

Where

$$C'_i = \frac{8.64 \times 10^4}{6.93 \times 10^{-1}} T_i C_i = 1.25 \times 10^5 C_i T_i (\text{rad / curie inhaled}) \quad (14.49)$$

For the thyroid gland the dose conversion factor is

$$\begin{aligned} C'_i &= \frac{(1.25 \times 10^5) (5.92 \times 10^2) (f_a) E T_i}{M} \\ &= \frac{7.40 \times 10^7 f_a E T_i}{20} = 3.7 \times 10^6 f_a E T_i \quad (14.50) \end{aligned}$$

The numerical values which are used in Equation (14.45), as well as the dose conversion factor, C'_i , are given in Table 14.8-6.